Cherenkov radiation-ring spectrometers in accelerator experiments

A. I. Ronzhin

Institute of High Energy Physics, Serpukhov

Fiz. Elem. Chastits At. Yadra 18, 1125–1161 (September–October 1987)

Detectors which detect the ring of Cherenkov radiation are considered together with their use in accelerator experiments.

INTRODUCTION

The identification of particles is one of the most important tasks in high-energy physics. One of the most general and difficult problems is that of particle identification in multiparticle production of secondary particles, for example, in $p\bar{p}$ or e^+e^- collisions.[1-3] This requires the simultaneous separation into species of several tens of particles in wide momentum and angular intervals. Among the instruments designed to solve this problem, a special position is occupied by Cherenkov radiation-ring spectrometers, which make it possible to identify particles by their velocity if there is an independent determination of their momentum or total energy.

In this review, we consider the operation of these detectors, the fields of their application, and the prospects for their use.

The review consists of three parts. The first considers ring spectrometers in which the photon detectors are multistage proportional and drift chambers with photosensitive additions. The spectrometers built and already used in fixed-target accelerators and in colliding beams are described. In the second part, the spectrometers in which the photon detectors are ionization-sensitive vacuum photon detectors are considered. The third part is devoted to the elaboration and prospects of the use of the method.

Principles of operation of the spectrometers and basic relations

Despite a great existing variety in the constructions of the spectrometers, their basic elements are a radiator, in which Cherenkov radiation is generated when a particle passes through it, a spherical mirror, which focuses the radiation into a ring, and a position-sensitive photon detector, placed in the focal plane of the spherical mirror. The quantities measured for single-charge particles are the radius of the ring and the position of its center, these being quantities that are uniquely related to the speed of the particle and the inclination of its path to the spectrometer axis. Thus, each particle can be identified in the spectrometers by its velocity if there is an independent measurement of its momentum or total energy.

Let us consider the basic relations for spectrometers with a spherical focusing mirror. The fundamental relationship for Cherenkov radiation is

$$\cos\Theta = 1/\beta n, \tag{1}$$

where θ is the angle of emission, β is the particle velocity, and n is the refractive index of the radiator. The connection between the radius r of the ring in the focal plane and the angle θ is[1)]

$$r = f \operatorname{tg}\Theta, \tag{2}$$

where f is the focal length of the spherical mirror. The displacement d of the center of the ring relative to the spectrometer axis, which coincides with the axis of the spherical mirror, is

$$d = f \operatorname{tg}\alpha, \tag{3}$$

where α is the angle of inclination of the path of the particle to the axis of the spherical mirror. The velocity resolution of the spectrometers is given by

$$\left(\frac{\Delta\beta}{\beta}\right)^2 = \left[(\operatorname{tg}\Theta\cdot\Delta\Theta)^2 + \left(\frac{\Delta n}{n}\right)^2\right] \Big/ N_0 L \sin^2\Theta, \tag{4}$$

where $\Delta n/n$ is the dispersion of the refractive index of the radiator, L is its length, and N_0 is the quality of the spectrometer, an important parameter that determines the quality of its optics and the photon detector:

$$N_0 = 2\pi\alpha z^2 \int_{\lambda_1}^{\lambda_2} \left(1 - \frac{1}{\beta^2\cdot n^2(\lambda)}\right) \frac{k(\lambda)\cdot\varepsilon(\lambda)}{\lambda^2}\, d\lambda, \tag{5}$$

where $\alpha = 1/137$, z is the charge of the particle, $k(\lambda)$ is the quantum efficiency of the photon detector, and $\varepsilon(\lambda)$ is the light transmission coefficient of the optical system. The number of photoelectrons detected per radiation ring can be written in the form

$$N_{\text{phe}} = N_0 L\cdot\sin^2\Theta. \tag{6}$$

We should also mention another relation that is helpful in calculations:

$$\Theta^2 = 2\,(\Delta n - \Delta\beta), \quad \Theta,\ \Delta n,\ \Delta\beta \ll 1. \tag{7}$$

Note that the velocity resolution of Cherenkov spectrometers depends on the accuracy of measurement of the emission angle and the dispersion of the refractive index of the radiator, and also on the number of photoelectrons detected per radiation ring.

The basic physical quantities that cause spreading of the rings and thereby determine the accuracy with which the emission angles can be found are as follows:

1. Dispersion of the refractive index of the radiator. The spreading of the emission angle due to this factor is

$$\Delta\Theta_{\text{ri}} = \frac{dn/dE\,\Delta E}{\sqrt{12}\, n \operatorname{tg}\Theta}, \tag{8}$$

where dn/dE is the change of the refractive index over the range ΔE of energies of the detected photons.

2. Multiple scattering of particles in the matter of the radiator. This is given by

$$\Delta\Theta_{\text{ms}} = \frac{15}{\beta pc}\sqrt{\frac{L/2}{X_0}}. \tag{9}$$

3. Spatial resolution σ_{sr} of the photon detector. This is given by

 0090-4759/87/050480-16$04.40

$$\Delta\Theta_{sr} = \sigma_{sr}/f. \quad (10)$$

4. Optical aberration. Aberration effects arise from the difference between the path distances to the photon detector for photons emitted from different points of the particle's path (for optical systems with a spherical mirror). These are

$$\Delta\Theta_{opt} \simeq \Theta^3. \quad (11)$$

5. Other factors. Among the other factors of a definite nature one can include the change in the emission angle due to energy losses in the radiator, the influence of a temperature gradient on the refractive index, a shift of the emission angle due to a change in the particle path in a magnetic field, etc.

1. SPECTROMETERS WITH GAS POSITION-SENSITIVE PHOTON DETECTORS

Gas photon detectors began to be widely used after the work of Sequinot and Ypsilantis,[4] who suggested that photon coordinates should be detected by a drift chamber containing saturated vapors of compounds with a fairly low photoionization potential. Photon detectors began to develop in two main directions after triethylamine (TEA) and tetrakis (dimethylamino) ethylene (TMAE) started to be used as photosensitive additives.[5,6] One direction was associated with the development of photon detectors based on two-coordinate drift chambers,[7] and the other with the use of multistage proportional chambers.[8] Thus, once the suggestion had been made in Ref. 4, the possibility was opened up of exploiting the entire developed power of the method of proportional and drift chambers—the achieved level in the technology of preparation and the large areas and high spatial resolution—for detecting Cherenkov radiation rings.

Let us compare the properties of TEA and TMAE. Figure 1 shows their quantum efficiencies, and also the transmission spectra of some gases and optical glasses.[9] It can be seen that the sensitivity range of TEA is the wavelength range 140–160 nm, and this limits its use to basically the noble gases and optical elements based on CaF_2, MgF_2, and LiF, which are transparent in the vacuum ultraviolet region. In contrast, TMAE can be used with quartz optics and a much greater variety of gas radiators. This is an important advantage of TMAE. Among the existing difficulties in the detection of radiation rings in the TEA photoionization region we must mention the poorer reflecting properties of the mirrors, the significant influence on photon absorption of oxygen and water impurities (their level must not exceed 10^{-6}), and the strong growth in the dispersion of the gas radiators in this region. It should also be emphasized that the mechanical properties of optical glasses made from CaF_2, MgF_2, and LiF permit them to be used in spectrometers at pressures of the gas radiators near atmospheric pressure.

The main shortcoming of TMAE is its low saturated-vapor pressure, which is 0.2 mm Hg at 20 °C (56 mm Hg for TEA), in connection with which the photon mean free path is about 15 mm (1 mm for TEA). This makes it necessary to increase the size of the conversion region to 45–60 mm (in the case of TMAE), as a result of which the photon detector becomes sensitive to the background of passing charged particles (the signal from charged particles is about 200 times greater than the signal from an individual photon). Besides this, serious difficulties arise with the suppression of the optical feedback which occurs because of the conversion of photons that are formed by gas multiplication and penetrate into the working region of the photon detector. One further shortcoming of TMAE is that it is readily oxidized, and this makes its use difficult.

We note that the detection of the vacuum ultraviolet is difficult, since it requires the creation of a fairly complicated system to control the purity of the gas radiator, the gas filling of the chamber, long-term stability, etc.[10]

Constructional details of photon detectors

We first consider photon detectors based on a two-coordinate drift chamber, shown schematically in Fig. 2. The volume of the chamber is separated from the gas radiator by an optical window made of a transparent material. The Cherenkov photons produced in the radiator pass through the window and are converted in the drift gap into photoelectrons, which then drift to the region of the proportional chamber, where they undergo gas multiplication. One coordinate of the photoelectron, usually taken to be Y, is determined by the drift time, and the other, X, by the number of the wire that responds in the proportional chamber. Figure 3 shows schematically one of the early chamber constructions.[5] A potential distributed uniformly in the direction of the drift is created by means of field-shaping wires placed with equal steps on both sides of the drift gap. Investigations made at an early stage[10] showed that field-shaping wires must also be placed on both sides of the entrance window in order to eliminate the loss of efficiency in photoelectron detection over the length of the drift gap. Losses were due to polarization of the windows and the distortions of the electric field that arose as a result.

One of the main problems in detectors of this type was optical feedback, which led to a large background in the chambers. It led not only to a significant number of re-

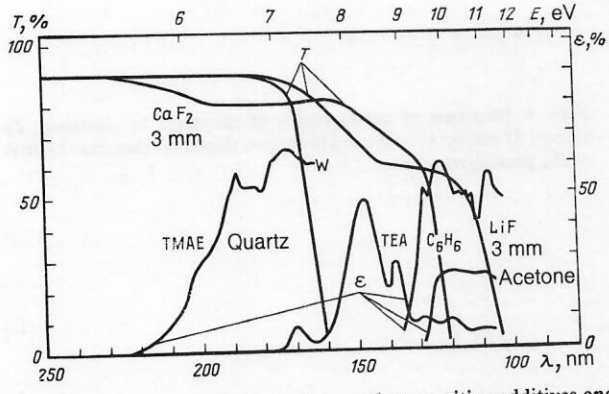

FIG. 1. Quantum efficiency ε of some photosensitive additives and light transmission T of different windows.

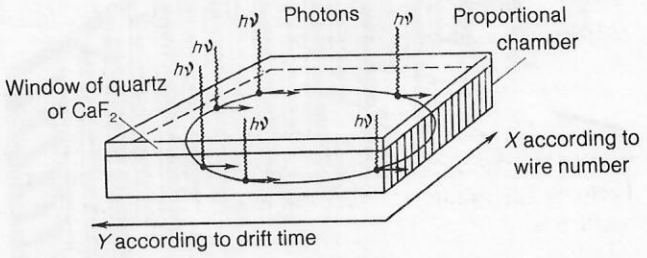

FIG. 2. Schematic diagram of two-coordinate drift chamber.

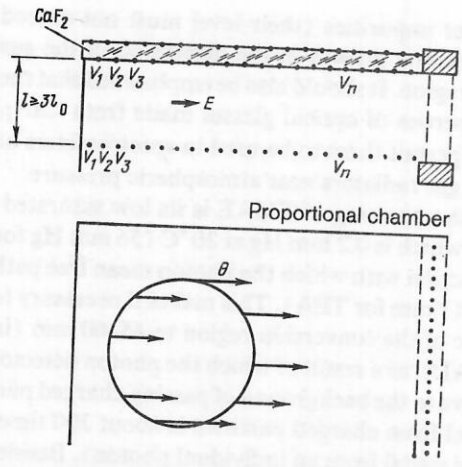

FIG. 3. Schematic representation of chamber construction (l_0 is the photon mean free path).

sponses from neighboring wires but also to background responses in the region of the photosensitive volume. This made it much harder to reconstruct the rings. The problem was attacked by several groups, and this resulted in the determination of some constructional features of the chambers. The feedback can be suppressed by placing screens near the anode wires or by introducing additional focusing electrodes and an additional drift gap, which divided the gas multiplication process into two stages and also made it possible to reduce the ion feedback (Fig. 4).[11] An additional means is the introduction into the gas mixture of additives that absorb part of the photon spectrum from the vacuum ultraviolet region. The problem of the optical feedback can now be regarded as solved.

The basic parameters of these photoelectrodes can be taken to be the following: the length of the drift gap, 20–150 cm (the corresponding total drift time is 2–15 μsec), the gas filling—methane or methane mixed with isobutane (high drift velocity, small electron diffusion coefficient, high gas multiplication, and good optical transparency), the spacing of the anode wires in the proportional chamber, 1–2 mm, and the gas multiplication: 10^5. A photon detector with these parameters and sensitive area measuring 1×1 m^2 contains up to 1000 signal wires and the same number of channels of the readout electronics. Each channel contains a low-noise amplifier–shaper and a time-to-digital converter. We note that such a photon detector has 10^6 discretely resolvable positions.

A photon detector based on a multistage proportional chamber was developed and investigated in great detail by Charpak's group.[12] It is shown schematically in Fig. 5. It contains an entrance window and a multistage proportional chamber divided by means of electrodes into several intervals for: conversion (C), preamplification (PA), transmission (T), and proportional amplification (PC). In the last the three projections of the photon coordinates are measured: U by means of the number of the anode wire, and X and Y by means of the charge induced on cathode wire electrodes arranged at right angles to each other and at 45° to the anode wires. Features of the chamber are the division of the amplification process into two stages, the presence of the transmission interval, and the way in which the signal electrodes are arranged. The advantages of the construction are the high gas multiplication (up to 10^7), the suppressed feedback, the localization of the avalanche in the gas multiplication process, and the possibility of controlling the chamber through the presence of the transmission interval. In the chamber model described in Ref. 13, four CaF_2 windows, each measuring $100\times100\times4$ mm, were used. This window size was chosen as a prototype for a working photon detector of area 800×400 mm^2, and therefore particular attention was devoted to the construction of the window supports. A solution that ensured hermetic sealing and eliminated the possibility of damage to the windows through thermal deformation was found. Each window of area 100×100 mm^2 was glued along the perimeter to a square steel tube of the same section with a wall of thickness 100 μm. The other side of the tube was glued into a recess in the supporting frame (Fig. 6). Figure 6 also shows the interelectrode separations in the chamber and typical distributions of the potentials on the electrodes. In the interval C there is conversion of the electrons, which are multiplied initially by up to 10^3 in the interval PA. Then the electron avalanche is transported through the interval T to the region of the proportional chamber PC, where the gas multiplication is up to 10^4. With allowance for the loss of electrons in the transmission interval the total gas multiplication may reach 10^7. The electrodes in the various intervals—conversion, preliminary multiplication, and

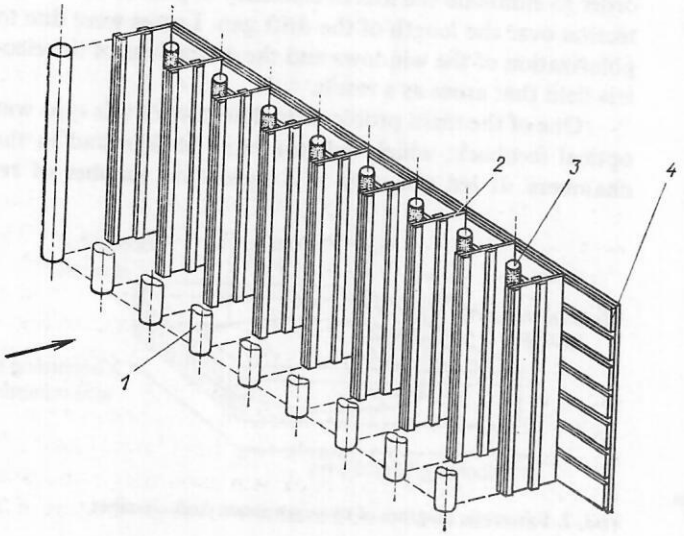

FIG. 4. Structure of anode region of chamber: 1) electrode; 2) screen; 3) anode; 4) cathode (the arrow shows the direction of drift of the photoelectrons).

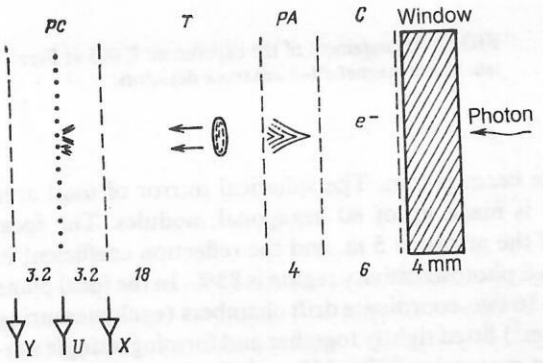

FIG. 5. Schematic arrangement of a photon detector based on a multistage proportional chamber.

transport—are made in the form of grids of nonrusting wires (wire diameter 50 μm, spacing 500 μm). The first grid is as close as possible to the CaF_2 window. The cathode electrodes of the proportional chamber are made of a copper–beryllium wire of diameter 50 μm with the wires separated by 1 mm, and the anodes are made of gilded tungsten wire of diameter 20 μm. The gas filling was a mixture of 97% He and 3% TEA, and also a mixture of 87% He, 10% CH_4, and 3% TEA. Information about the position of incidence of a photon in the chamber was read out in three projections, X, Y, and U, by means of analog-to-digital converters connected to each signal electrode; for the cathode electrodes the coordinates were measured by the method using the centroid of the induced charge. Subsequently, the cathode electrodes were combined into groups of three each, since the required accuracy was then ensured. In the X and Y projections, the spatial accuracy ($\sigma_{X,Y}$) in the determination of the photon coordinates was 0.4 mm; in the U projection, the accuracy was determined by the spacing of the anode wires (1 mm). Pulse-height information from the electrodes was used to "match" the coordinates of the given photon in the three projections.

We now list the advantages and shortcomings of these photon detectors. Among the advantages of the multistage chambers, the main ones are the high gas multiplication, the suppressed feedback, and the short dead time, which is determined by the spread of the photon conversion time and is 50 nsec when TEA is used. Shortcomings of the photon detector are the impossibility of reconstructing more than one ring in the complete working region; moreover, the number of points on the ring must not exceed five.[14] This is due to the information readout system, and the authors hope that the use of fine-structure cathode electrodes will make it possible to eliminate this shortcoming. Apart from this the "quality" of the multistage proportional-chamber photon detectors is 2–3 times lower than that of the photon detectors based on two-coordinate drift chambers; in addition, from the mechanical point of view the multistage detectors are much more difficult to use than the two-coordinate drift chambers in the complicated configurations—ring-shaped, spherical, etc.—needed in colliding-beam facilities. Undoubted advantages of the two-coordinate drift chambers are the possibility of detecting events with a high multiplicity of rings, the comparative economy of the electronics, and the weaker demands on the optics (when TMAE is used). Shortcomings of the photon detectors based on two-coordinate drift chambers are the relatively long dead time, the loss of photoelectrons in the case of large drift gaps, and the high sensitivity to charged particles. The most important advantage of the photon detectors is the possibility of covering large areas with a high spatial resolution for individual photons, and shortcomings are the difficulties mentioned in connection with the detection of photons from the vacuum ultraviolet region.

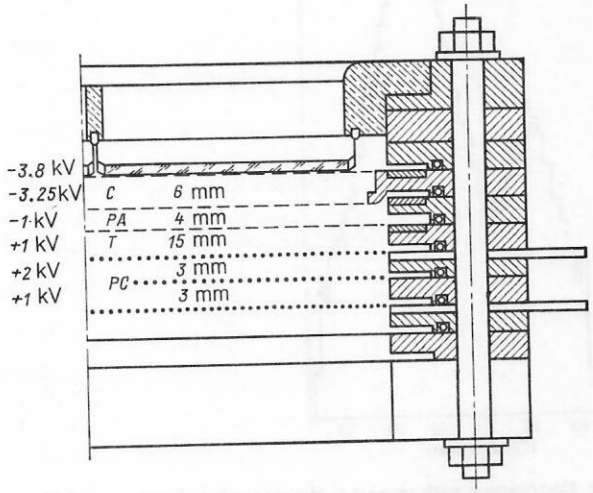

FIG. 6. Chamber construction.

Working ring spectrometers with photon detectors based on chambers and ones near completion

We shall now consider spectrometers that are already being used in experiments, and also ones that are near completion.

Historically, the first spectrometer with a multistage proportional chamber as a photon detector was created by Charpak's group and used in experiment E 605 at Fermilab.[16,18] The facility (Fig. 7) was designed for the investigation of hard processes of production of particles with large transverse momenta. One of the main detectors in the facility is RICH (Ring Imaging Cherenkov Counter), which is used for the identification of pions, kaons, and protons in the range of momenta up to 300 GeV/c. For this a velocity resolution not worse than 10^{-6} is required. It was achieved by using helium at atmospheric pressure as a gas radiator and by increasing the length of the radiator to 15 m. The radiator was put in two adjoining volumes measuring $2\times2\times7$ and $3\times3\times8$ m^3 of total length 15 m. At the end of this region there was a spherical mirror of area 2.5×2.5 m^2 consisting of 16 sections. Each of the halves of the mirror, measuring 1.25×2.5 m^2, focused the Cherenkov radiation in two directions symmetric with respect to the spectrometer axis. The focal distance of the spherical mirror was 8 m. The reflection coefficient of the mirror in the region of TEA photoionization was 75%. In the focal plane of each of the halves there were two photon detectors based on multistage proportional chambers, each having an area 800×400 mm^2. The dependences of the number of photoelectrons and the ring radii on the momentum in a given spectrometer are shown in Fig. 8. Figure 9 shows the measured distribution with respect to the radius of the rings for pions and kaons with momentum 200 GeV/c. The FWHM of the distribution for the pions is 0.9 mm ($N_0 = 24$), approximately two times lower than in the tests with a model because of oxygen impurities in the radiator and also the need to add methane to the gas mixture of the

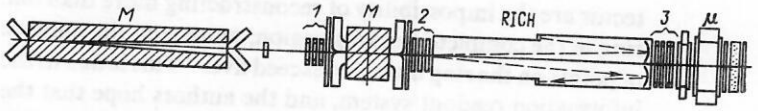

FIG. 7. Arrangement of the experiment E 605 at Fermilab: M are magnets; 1–3 are track detectors.

photon detector to cut off the region of the spectrum with large dispersion of the refractive index. The emission angle for particles with $\beta = 1$ was 8.7 mrad, and each of the halves of the spectrometer covered an angular area of 50×100 mrad. Statistics collection occurred under conditions of detection of not more than three points per ring for particles with $\beta = 1$. The detection efficiency was 95%. The identification of the pions and kaons in the region of maximal momenta was realized at the 90% confidence level. For the identification, information was used about the number of particles (not more than one for each photon detector) and the path parameters and momentum, obtained from track detectors and by magnetic analysis. The detector was equipped with a control system for transmission of the gas mixture and the radiator and was used at a pressure slightly above atmospheric. This spectrometer was the first and, as yet, the only one in which a multistage proportional chamber was used as a photon detector. Its designers believe that its characteristics can be improved.[19–21] The constructional features of the spectrometer are typical of experiments with a fixed target at high energies.

At the present time, the only working spectrometer with a two-coordinate drift chamber as a photon detector is used in the experiment WA-69 at CERN.[15] A feature of this huge detector (Fig. 10) is the possibility of simultaneous identification of particles in a wide momentum range (pions and kaons with momenta from 10 to 160 GeV/c) with a large working angular and radial aperture (angles relative to the spectrometer axis up to 30°, transverse dimensions 4×2.5 m^2); moreover, the particles are produced in the final state with high multiplicity in the photoproduction process. As a radiator, the spectrometer uses nitrogen at atmospheric pressure (refractive index in the TMAE sensitivity range equal to 1.00031–1.00035); the length of the gas radiator along the beam is 5 m. The spherical mirror of total area 7×4 m^2 is made up of 80 hexagonal modules. The focal length of the mirror is 5 m, and the reflection coefficient in the TMAE photosensitivity region is 85%. In the focal plane there are 16 two-coordinate drift chambers (each measuring 80×40 cm^2) fitted tightly together and forming a single sensitive area measuring 320×160 cm^2. Each such photon detector is separated by a proportional-chamber region into two halves measuring 80×20 cm^2 (20 cm in the drift direction). The separation of the wires in the proportional chamber is 4 mm. Each of the wires is separated from its neighbors by screens. The two-coordinate drift chambers are fitted with 32 quartz windows, each measuring $80 \times 20 \times 0.3$ cm^3. The gas filling employed is a mixture of 80% methane, 20% isobutane, and saturated TMAE vapor. To ensure effective conversion of the photons, the depth of the two-coordinate drift-chamber photon detector is 50 mm. Figure 11 shows the radii of the rings for pions, kaons, and protons as functions of the momentum. The spreading of the rings for an individual photoelectron in units of σ is due to the dispersion of the refractive index of the gas radiator (1.8 mm); the contribution of the optical aberration is 1 mm, and the contribution of the spatial resolution of the photon detector is about 1 mm. The total spatial resolution for an individual photon is 3 mm. In the design of the spectrometer $N_0 = 90$ was taken; experimentally, $N_0 = 40$ was obtained. The mean detected number of points per radiation ring for particles with $\beta = 1$ is 16, and this gives an accuracy in determining the ring radii of 0.7 mm. Figure 12 shows the distribution with respect to the radii of the rings for pions and protons with momentum 100 GeV/c. Figure 13 shows an event in the spectrometer corresponding to an initial photon with energy 170 GeV (the mean multiplicity of particles in an event is 7).

In the photon detector, 3200 signal wires are used. Each

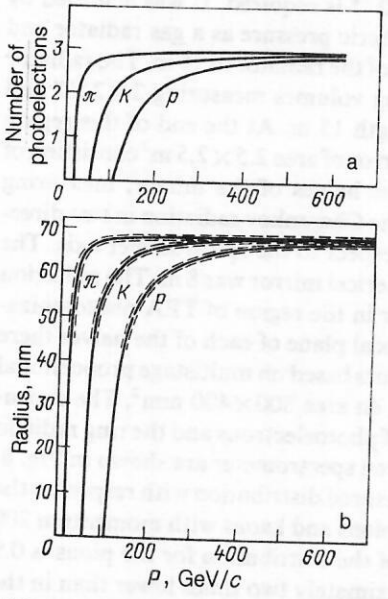

FIG. 8. Number of photoelectrons (a) and ring radii (b) as functions of the momentum for pions, kaons, and protons.

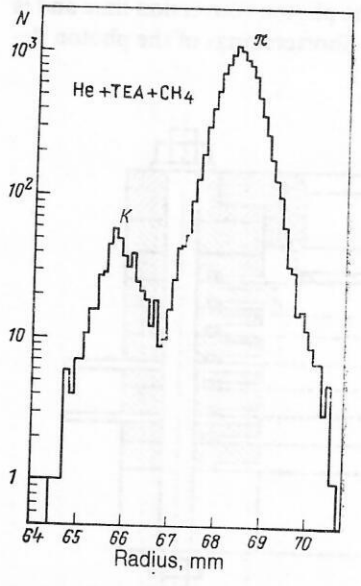

FIG. 9. Distribution with respect to the ring radius for pions and kaons with momentum 200 GeV/c.

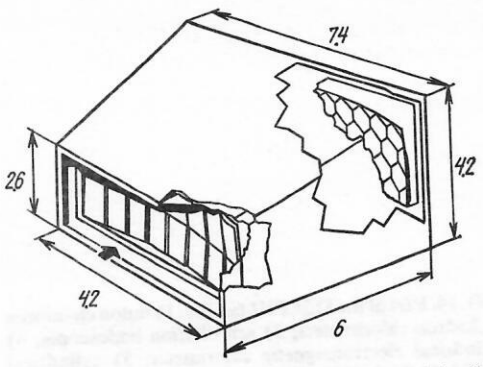

FIG. 10. The RICH spectrometer in the Omega (the dimensions are given in meters).

detection channel contains a low-noise amplifier with gain 200 an amplifier/discriminator, and a time-to-digital converter. In each time-to-digital converter, shift registers are used; these have a strobing time corresponding to 4 mm in the chamber space and are connected to a cyclic memory of 192×64 bits (192 for the numbers of the wires of the module of the two-coordinate drift chamber and 64 for measuring the drift time with respect to each channel). At a time 500 nsec after the firing of the trigger for an interaction with a high multiplicity the registers are stopped, and after 2.5 μsec information from the cyclic memory is read out. It is then decoded and transferred to a 18-bit memory (12 bits for the numbers of the wires for the complete photon detector and 6 bits for time information). It is proposed later to use a multilevel processor to which information will be sent from the track detectors about the number of particles and their paths. In the matrices of the memory, this information will make it possible to determine the momenta of the particles and the centers of the rings for them. The following matrix, which has a mass hypothesis within it, predicts the radii of the rings and the number of expected points in each of them. The information is then compared with that obtained from the spectrometer, and a decision is made about whether or not to actuate the trigger for readout of all the information from all the remaining detectors. According to calculations, the trigger generation time must be 52 μsec.

The method with two-coordinate drift chambers as photon detectors proved to be very promising under conditions of not too high load of the facility (for the Omega spectrometer the flux of photons in the experiment did not exceed 10^4 sec^{-1}), ensuring unique conditions for covering huge areas in a complicated configuration of photon detectors. In this connection, it can be widely used in facilities with colliding e^+e^- beams. There is in this case, in contrast

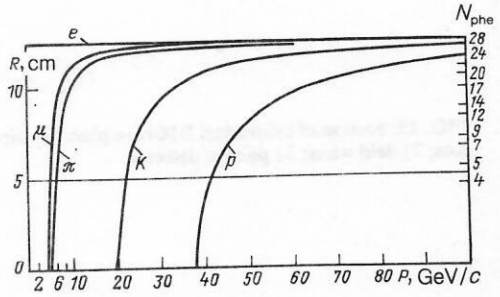

FIG. 11. Number of photoelectrons and ring radii for muons, pions, kaons, and protons as functions of the momentum.

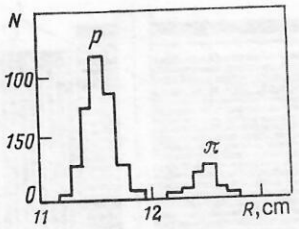

FIG. 12. Distribution with respect to the ring radius for pions and protons with momentum 100 GeV/c.

to hadron colliders, one further condition for its successful use. The point is that the restricted size of the facilities makes it impossible to use long gas radiators (longer than one meter) for the identification of secondary particles (π,K,p) with momenta of several tens of GeV/c, but the secondary hadrons in the e^+e^- colliders that have been developed have a mean momentum of not more than 20 GeV/c. This range can be well covered if one uses in the spectrometers thin liquid[2)] radiators (about 1 cm), and also gas radiators not longer than 1 m. Possessing a high angular resolution (for effectively 4π geometry) and the possibility of detecting events with high multiplicity in a wide momentum range, ring spectrometers with two-coordinate drift chambers as photon detectors have been given a special place in the planned LEP[3] and SLAC[17] facilities.

Figure 14 shows part of the DELPHI facility, which is symmetric with respect to the position of collision of the e^+ e^- beams in LEP.[3] Within the superconducting solenoid with field directed along the beam, behind the central track system, cylindrical and end ring-imaging Cherenkov counters (RICH) are placed. The region occupied by the detectors in the radial direction is in the interval from 1.23 to 1.97 m, and in the direction of the beams it is 5.4 m. The cylindrical RICH contains in one space liquid and gas radiators; in the end RICH they are spatially separated. The liquid radiators cover the polar angles from 15 to 41° and from 41 to 90°, and the gas detectors cover the polar angles from 12 to 38.5° and from 50 to 90° in the cylindrical and end parts of the detector, respectively. Thus, the liquid RICH covers 96.6% and the gas RICH 83.9% in the 4π geometry. Sections of the cylindrical RICH in plan and in the transverse direction are shown in Figs. 15 and 16. In the azimuthal direction, the RICH is divided into 36 identical sections with respect to the position of collision of the e^+e^- beams (altogether 72 sections). Each section contains a two-coordinate drift chamber as a photon detector, on the basis of which both the gas and liquid radiators work. In the volume of the gas radiator four spherical mirrors (in each of the sections) focused on the photon detector are placed. The transverse dimensions of the photon detector and of the liquid radiator in each section are 1.45×0.25 m^2; the depth of the photon

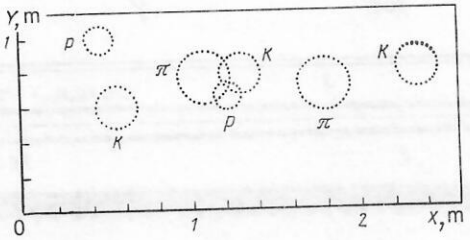

FIG. 13. Typical event in RICH.

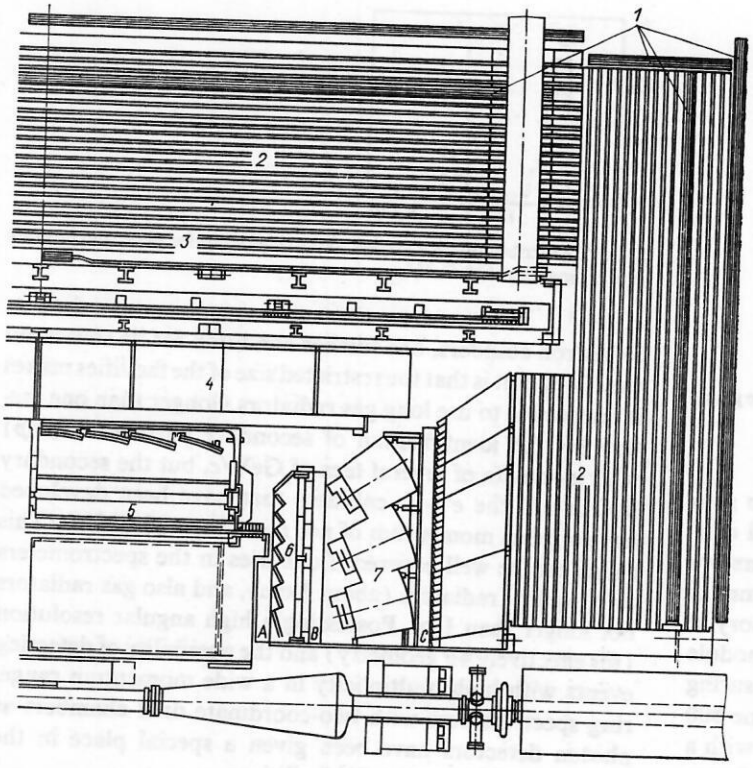

FIG. 14. Part of the DELPHI facility: 1) muon chambers; 2) hadron calorimeters; 3) scintillation hodoscopes; 4) cylindrical electromagnetic calorimeter; 5) cylindrical RICH; 6) liquid RICH; 7) gas RICH.

detector increases smoothly from 45 to 60 mm in the direction of drift of the photoelectrons, the region of the proportional chamber being situated at the end of the drift region. This construction is chosen in order to decrease the influence of the radial component of the solenoid field on the drift of the photoelectrons. The wires of the proportional chamber are separated by screens. Each two-coordinate drift-chamber module contains 91 signal wires of diameter 20 μm with the wires separated by 2.54 mm. Near the signal wires is a cathode plane, segmented into 12 parts over the depth of the two-coordinate drift chamber and into three in the azimuthal direction, forming 36 cathode areas. The coordinate of the photon conversion in the direction of the depth of the photon detector is measured in order to increase the accuracy in the determination of the ring radii. Quartz windows of thickness 5 mm and a gas mixture of 80% methane, 20% isobutane, and saturated TMAE vapor at 40°C are used. The gas radiator is FC 87 ($T = 40$ °C), and the liquid radiator is FC 72. The refractive indices are 1.0018 and 1.26, respectively. Altogether, the cylindrical RICH contains 72 photon detectors, 288 mirrors, 6552 signal wires, and 2592 cathode areas.

The gas end RICHs contain 88 separated regions, each with its own mirror and photon detector. The focal length of the mirror is 48 cm. The radiator is FC 87. The liquid end RICHs are spatially separated from the gas RICHs and work with their own photon detectors. In the gas RICHs there are 3300 readout channels for the signal electrodes and 550 for the cathode electrodes. The readout electronics, developed in the standard FASTBAS, has parameters close to those used in the Omega spectrometer.[22] The design parameters of the RICHs are as follows:

Liquid radiator:	FC 72
refractive index	1.26
Gas radiator:	FC 87, $T = 40$ °C
refractive index	1.0018

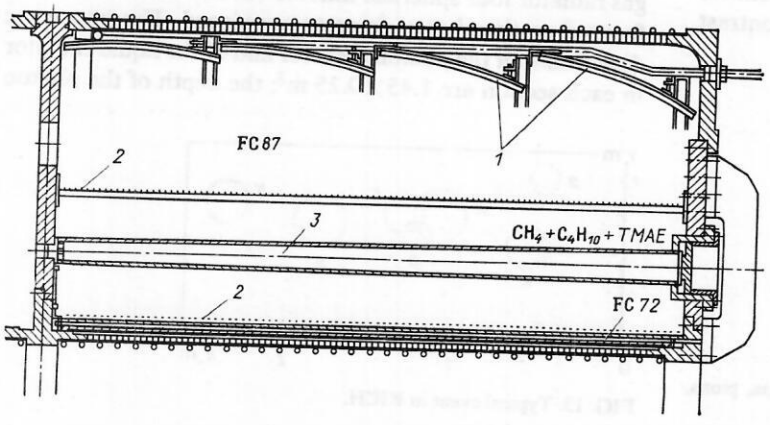

FIG. 15. Section of cylindrical RICH in plan: 1) mirrors; 2) field wires; 3) photon detector.

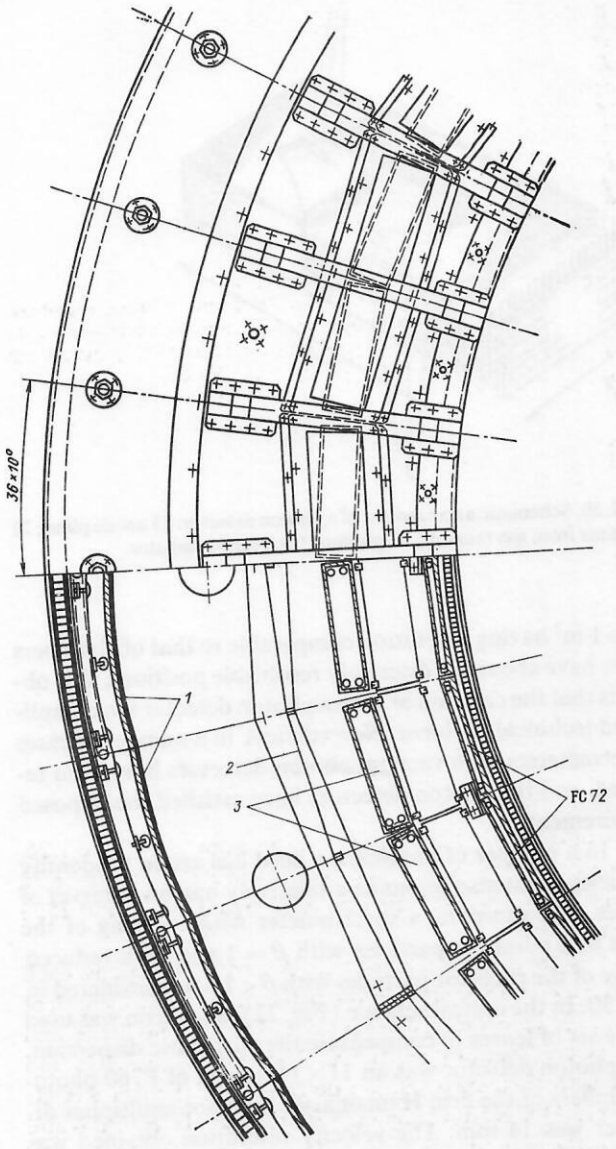

FIG. 16. Section of RICH in the transverse direction: 1) mirrors; 2) field wires; 3) photon detector.

Length of gas radiator, cm .....Up to 60
Thickness of liquid radiator, mm:
of cylindrical RICH 10
of end RICH 15

Velocity resolution:
of gas RICH .....10^{-4}
of liquid RICH .....10^{-3}
Number of photoelectrons:
of gas RICH .....Up to 13
of liquid RICH .....Up to 20

When information about the momenta and paths of the secondary particles is used, the RICH must ensure identification of pions, kaons, and protons in the momentum range 2–20 GeV/c. As an illustration, Fig. 17 shows a typical expected example of an event with two hadron jets.

The RICH being currently developed for the SLD facility on the SLC[23] is basically similar, and we therefore give only individual details for it. In the cylindrical part (Fig. 18) two-coordinate drift chambers as photon detectors are used, four each along the length, with drift gap 80 cm and width 20 cm. The end RICHs are distinguished by having the liquid and gas radiators, which work with a common photon detector (Figs. 19 and 20), in a common space. A constructional feature of the photon detectors is the configuration of screens at the anode wires and the introduction of an additional drift gap to suppress feedback (Fig. 21). Full-scale testing of the photon detector in a model has already been done.[24] A value $N_0 = 94$ and spatial resolution 1.5 mm with respect to the drift coordinate for drift gap 80 cm were obtained. The authors note the occurrence of a problem in the form of a serious loss of photoelectrons due to the drift gap. Losses of 2.71 times occur over the length of 30 cm, and at present this is the main problem that needs to be solved.

Thus, it can be assumed that two-coordinate drift chambers as photon detectors have reached maturity and that their capabilities will be demonstrated once LEP and SLC have been commissioned.

2. SPECTROMETERS WITH VACUUM POSITION-SENSITIVE PHOTON DETECTORS

The first photographs of Cherenkov ring radiation were taken by V. P. Zrelov in a beam of 660-MeV protons and were demonstrated at the Nobel lecture of P. A. Cherenkov.[25] Later, the rings were detected by means of image converters developed in our country by M. M. Butslov.[26] The method of detecting the rings by means of vacuum photon detectors was, in essence, a further development of the method of gas differential Cherenkov counters.[27,28] An important

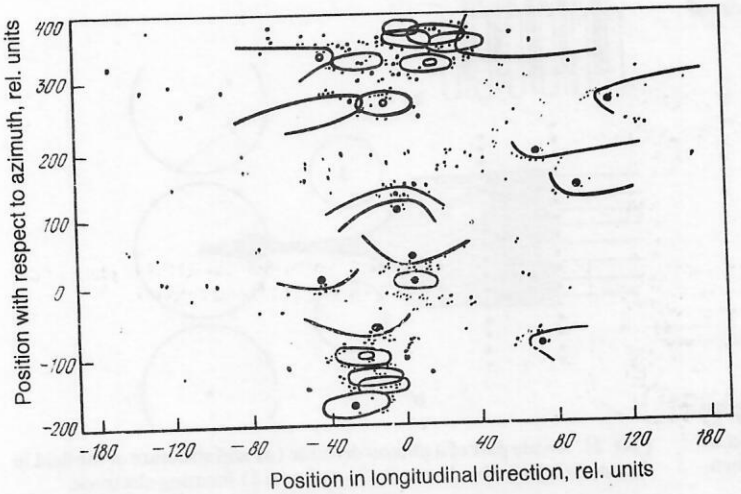

FIG. 17. Typical expected two-jet event.

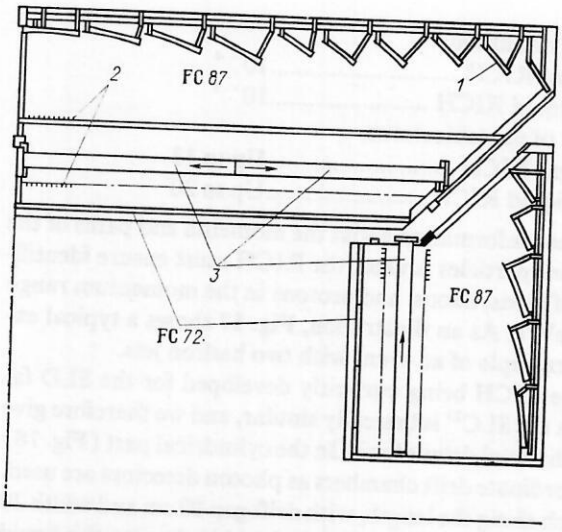

FIG. 18. The RICH of the SLD facility in the SLC: 1) mirror; 2) field wires; 3) photon detector.

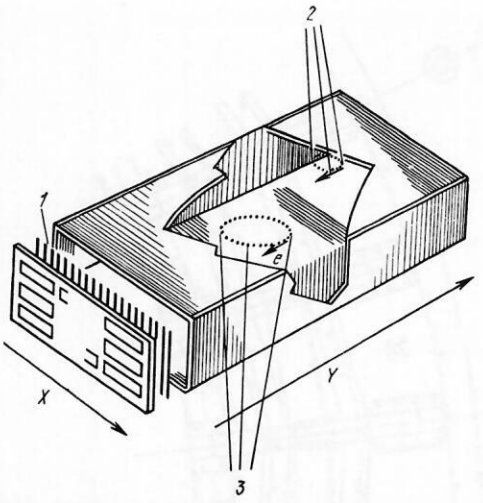

FIG. 20. Schematic arrangement of a photon detector: 1) anode plane; 2) photons from gas radiator; 3) photons from liquid radiator.

step in its realization was the replacement of the narrow ring diaphragm in the differential Cherenkov counter by a position-sensitive photon detector situated in the focal plane of a spherical mirror. Viewed historically, the direct predecessors of the ring spectrometers in the modern understanding were differential Cherenkov counters in which the photomultipliers scanned several concentric zones in the focal plane.[29]

Vacuum photon detectors have a number of undoubted advantages over photon detectors based on chambers. These include detection of the Cherenkov radiation in the visible region and the high quantum efficiency of the photocathodes corresponding to this region (up to 40%; we note that $N_0 = 100$ is a value long ago achieved for Cherenkov counters with photomultipliers), and also the faster response and the possibility of using in this connection a first-level trigger. Detection of the radiation in the visible region reduces the technical difficulties when gas radiators under pressure are used and simultaneously lowers the requirements on the optical elements and the control of the stability of their parameters; there is no need to use systems to purify gas mixtures that are "delicate" when photosensitive additives are handled, etc.

The absence of a vacuum position-sensitive photon detector of comparable size and coordinate resolution as the chamber-based photon detectors is the main obstacle to realization of the method. We recall that a photon detector of area 1 m^2 having resolution comparable to that of chambers must have about 10^6 discretely resolvable positions. It is obvious that the creation of such a photon detector is a complicated technical problem. Nevertheless, in a number of cases spectrometers with vacuum photon detectors have been realized, and the photon detectors have satisfied the imposed requirements.

In a number of problems, a need has arisen to identify particles in intense beams in a relatively narrow interval of angles. For example, a spectrometer with focusing of the rings to a point for particles with $\beta = 1$ and with reduced image of the rings for particles with $\beta < 1$ was considered in Ref. 30. In the optical scheme (Fig. 22), an axicon was used in the set of lenses to compensate the chromatic dispersion. The photon detector was an 11×11 matrix of P760 photomultipliers of the firm Hamamatsu; the photomultiplier diameter was 14 mm. The velocity resolution obtained was 1.4×10^{-5} (the contribution of optical aberration was 1.1×10^{-5}, and the spatial resolution of the photon detector was 0.5×10^{-5}) in an angular range of ± 3 mrad for emission angles up to 35 mrad (the radiator was a mixture of gases). The detector was able to discriminate pions and kaons up to 30 GeV/c. Later, Meunier[31] proposed an optical

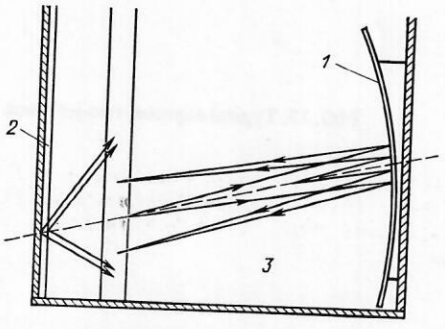

FIG. 19. Arrangement of part of a section of end RICH: 1) mirror; 2) liquid radiator; 3) gas radiator. The broken line shows the direction of motion of the particle, and the arrows show the direction of the radiation.

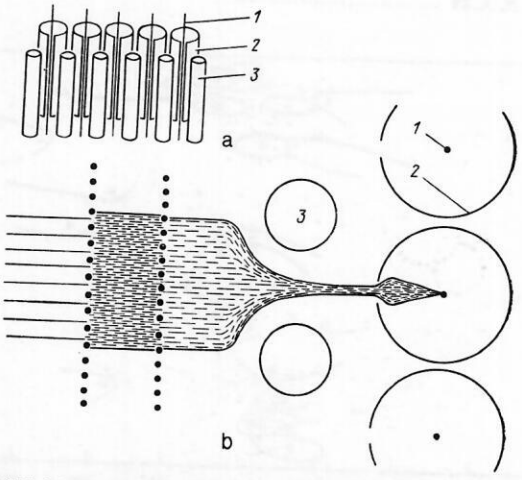

FIG. 21. Anode part of a photon detector (a) and structure of the field in the anode region (b): 1) anode; 2) cathode; 3) focusing electrode.

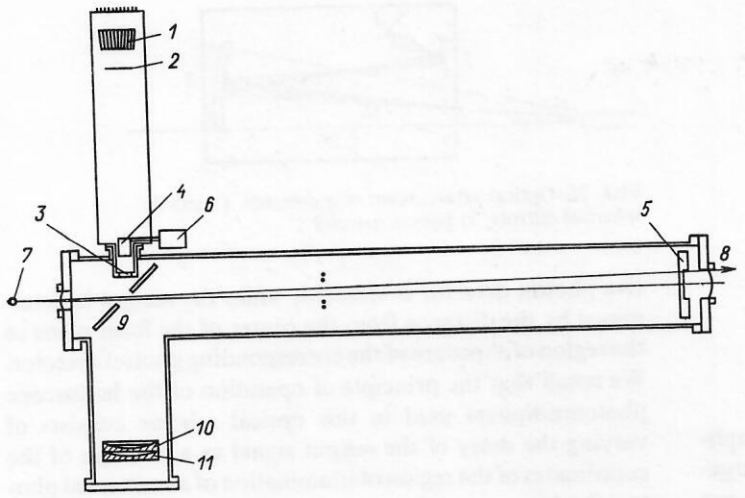

FIG. 22. Schematic arrangement of a ring detector: 1) matrix of phototubes; 2) field lenses; 3) optical window and field lens; 4) transfer lenses; 5) spherical mirror; 6) transfer lens monitor; 7) target; 8) particle; 9) flat mirror; 10) axicon; 11) spherical mirror.

scheme that makes it possible to enlarge the range of angles of the detected particles (Fig. 23). It needs to be emphasized that this optical scheme is suitable for small targets (diameter about 3 mm) and in the absence of magnetic elements between the target and detector. The optical scheme employs a spherical mirror with focal length F, and the image of the target in the mirror is behind the focal plane at the point T_1. At this point the first field lens L_1 is placed. Its position is chosen with allowance for the fact that for all particles emitted from the target at different angles the light rays are incident on the lens symmetrically, and its diameter determines, in particular, the range of detected emission angles. To remove the lens from the beam, a flat mirror is used. In principle, the placing of the lens L_1 ensures conditions of focusing of the rings with a reduction of their diameters, but the presence in the optical system of the lens L_2 makes it possible to vary the focal length in a wide interval. The use of a doublet of lenses with variation of the distance between them simplifies the conditions of focusing when different gas radiators are used and makes it possible to compensate the dispersion of the refractive index. Thus, the method of reducing the ring image makes it possible in a number of cases to extend the range of angles of the detected particles, ensuring at the same time an acceptable level of the necessary number of discrete vacuum photon detectors.

Another direction in the development of photon detectors is associated with hopes of using image converters in optical systems with reduction of the ring image. In the number of discretely resolvable positions, an image converter with an area of the working region of several tens of square centimeters and a resolution of about 30 pairs of lines per 1 mm is not inferior to the chamber-based photon detectors which we have been considering. Attempts to overcome their main shortcoming—the low counting rate—involve the search for fast scintillators and the realization of a control regime. One of the early experimental achievements in the detection of rings by means of a four-cascade image converter was reported by Giese *et al.*[32] They describe a 10-m Cherenkov chamber filled with He at atmospheric pressure in which a spherical mirror with focal length 10 m was used. A velocity resolution of 6×10^{-7} for selection of events with more than five points on a ring was achieved.

A combined photon detector using an image converter was realized by a group at Fermilab (experiment E 609).[33] The photon detector is shown in Fig. 24. It uses an image tube measuring 50×50 mm^2 with spatial resolution 50 μm. The spectrometer employs an optical scheme with image reduction containing two spherical mirrors (Fig. 25).

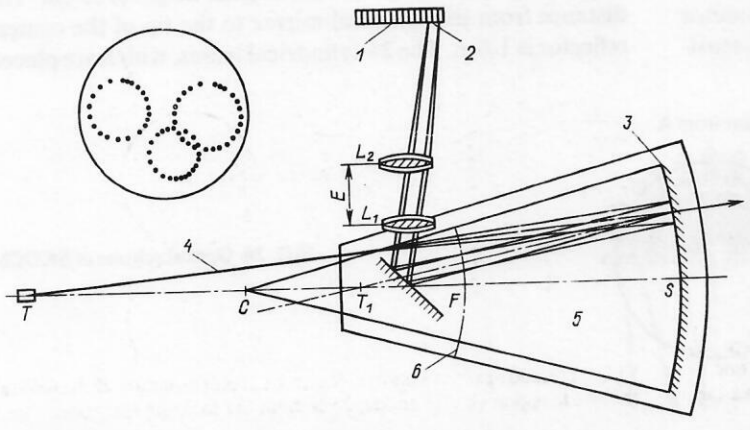

FIG. 23. Optical arrangement of a wide-aperture detector: 1) matrix of photomultipliers; 2) region of focusing of rings; 3) spherical mirror; 4) particle; 5) radiator; 6) focal plane.

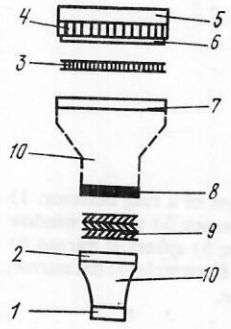

FIG. 24. Schematic arrangement of a photon detector.

The photon detector (Fig. 24) contains two light amplification cascades, the second being connected to a charge-coupled device (CCD) 1. Two amplification cascades are used to raise the signal above the CCD noise level. The photon detector contains an entrance quartz window 5, a fiber-optic disk 4, a photocathode 6, and a gap of amplification in a microchannel plate 3. A fast scintillator 7 with luminescence time 160 nsec is then used, together with the fiber-optic disk 10 to reduce the image, the image converter with photocathode 8, three microchannel-plate amplification cascades 9, and a scintillator 2 with luminescence time 2 μsec. Then comes one more fiber-optic disk 10, which directs the light to the CCD 1, which measures 12×12 mm^2 and has 390×244 elements. The authors note that the main difficulty in working with the photon detector was the instability of the microchannel plates, and for this reason, in particular, it was necessary to use several amplification cascades. A model spectrometer was built and tested, the photon detector working in a stable manner for 1000 h. The value $N_0 = 28$ was obtained. In the actual spectrometer it is hoped to discriminate pions and kaons with momenta up to 60 GeV/c. Among other proposals using multistage proportional chambers and image tubes in a spectrometer we may mention Ref. 34. The use of image tubes with trigger control is proposed.

With a view to reducing the number of photon detectors in the ring spectrometer, an optical scheme was proposed at the Institute of High Energy Physics at Serpukhov in which one-dimensional position-sensitive photon detectors are arranged along the radii of sectors in the focal plane of a spherical mirror. The photon detectors employed were the hodoscope photomultipliers proposed and developed at Serpukhov[36,37] as well as straight arrangements with discrete photomultipliers (FÉU 85).[38] In this optical scheme, one photon coordinate is determined by the number of the sector in which the corresponding one-dimensional position-sensitive photon detector is situated, while the second is determined by the distance from the center of the focal plane to the region of exposure of the corresponding photon detector. We recall that the principle of operation of the hodoscope photomultipliers used in this optical scheme consists of varying the delay of the output signal as a function of the coordinates of the region of illumination of an extended photocathode.

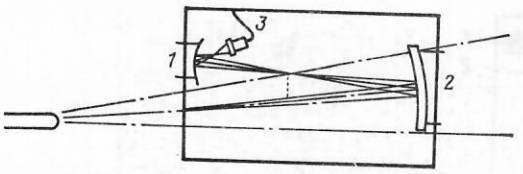

FIG. 25. Optical arrangement of a detector: 1) and 2) spherical mirrors; 3) photon detector.

The first ring detector based on hodoscopic photomultipliers was built and used in an experiment to observe antitritium nuclei.[39] Since then, progress has been achieved in the parameters of the hodoscope photomultipliers, and this has made it possible to use them as the basis of the wide-aperture ring spectrometer SKOCh[40] for the focusing double-arm spectrometer (FODS).[41] The spectrometer is designed to identify pions, kaons, and protons in a wide diverging beam in the momentum interval 5.5–30 GeV/c. The optical scheme of SKOCh is shown in Fig. 26. It contains a gas radiator 7, in which Cherenkov radiation is generated when a particle passes, a spherical mirror 6, which focuses the Cherenkov radiation into a ring in the focal plane, a conical reflector 5, which transforms the focal plane into a cylindrical surface, the cylindrical focusing lenses 4, the windows 3, which separate the volume of the gas radiator from the photon detectors, and the hodoscope photomultipliers 1 with specular air light guides 2. Thus, the radiation ring is divided in the focal plane into sectors, and the image of the part of the ring in each sector is transformed by means of the cylindrical lenses into a narrow region on the photocathode in the direction transverse with respect to the change in the delay of the hodoscope photomultipliers. Figure 27 shows a photograph of the exterior of the spectrometer. Its frame, designed to withstand a pressure of up to 10 atm, is made of a steel tube of diameter 1.2 m, to which collars of thickness 2 mm are joined at the place where the particle beam passes. The radiator is freon-13 at working pressure 5 atm. The active length of the gas radiator is 1.8 m. The diameter of the spherical mirror is 1.1 m, and the focal length is 2.5 m. The diameter of the base of the conical reflector is 70 cm, and the height is 35 cm. The distance from the spherical mirror to the tip of the conical reflector is 1.8 m. The 24 cylindrical lenses, which are placed

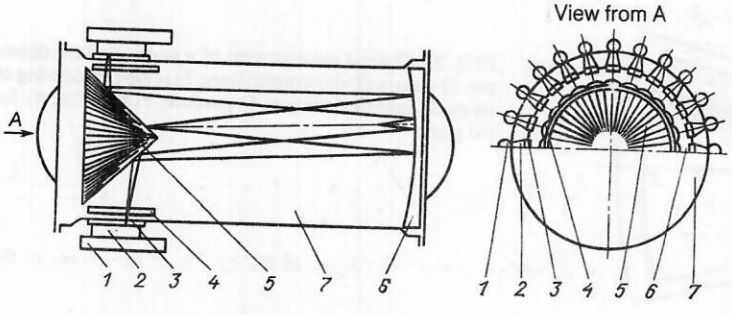

FIG. 26. Optical scheme of SKOCh.

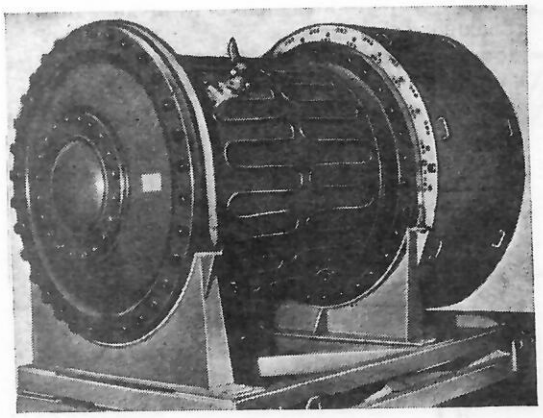

FIG. 27. Photograph of SKOCh.

tightly next to each other on a ring-shaped frame, form a cylindrical surface of diameter 80 cm. Outside the volume of the gas radiator, behind the exit windows, are 24 hodoscope photomultipliers with specular air light guides. These each contain two flat mirrors placed at 30° relative to each other; the entrance window of a light guide has area 200×40 mm^2, and the exit window, turned toward the photocathode of the hodoscope photomultiplier, has area 200×5 mm^2 (5 mm in the direction across the photocathode). The detecting system is based on electronics for information readout to the system SUMMA.[42] Each of the 24 detection channels contains a hodoscope photomultiplier, a fast amplifier (based on μA 733, voltage gain 10, transmission band up to 100 MHz), a shaper with slave threshold 6 UD-19 (Ref. 43) (accuracy of time matching $\pm$ 0.1 nsec in the range of input signals 5–500 mV), and a time-to-digital converter (TDC). Modified time–time converters[44] were used as TDCs. The amplifiers and shapers were placed in the immediate vicinity of the anode outputs of the hodoscope photomultipliers; this made it possible to reduce to a minimum the influence of external disturbance. A low noise level in the detection channel (10^3–10^4 sec^{-1} in the single-electron detection regime) was ensured by using hodoscope photomultipliers with bialkaline photocathodes, by optimizing the construction of the electrodes, and by the choice of appropriate supply regimes. The TDCs had channel division 1 nsec; the range of measured drift times was 500 nsec; the integrated nonlinearity of the TDCs did not exceed 0.5%, and the differential nonlinearity was less than 5%. One of the features of the employed modification of the TDCs was the placing of fast commutators at the inputs.

In each session, SKOCh was calibrated. This was done by establishing a correspondence between the coordinates of the points at which the photons struck the photocathodes of the hodoscope photomultipliers, expressed in digital codes, and the angles of the Cherenkov radiation in the spectrometer. Information about the momenta of the particles and the parameters of their paths, obtained from the system of drift chambers and by magnetic analysis, was used. The calibration was done with a definite mean value of the momentum with $\Delta p/p = 20\%$; for this value, because the beam contained several particle species and had an angular divergence, practically the entire range of angles of the Cherenkov radiation detected in SKOCh was covered. We give now the measured and design characteristics of SKOCh:

Pressure (freon-13), atm	5
Length of radiator, m	1.8–2
Focal length of mirror, m	2.5
Radial aperture, cm	40
Angular aperture, mrad	30
Range of emission angles, mrad	40–100
Number of detected photoelectrons:	
experiment	6–21
calculation	6–20
Experimental quality N_0	20–15 (40–30)*
Velocity resolution:	
experiment	$\pm 3\times10^{-5}$
calculation	$\pm (1.5\text{–}2)\times10^{-5}$
Number of detection channels (hodoscope photomultiplier, amplifier, shaper, TDC)	24

*After modification of individual elements of the optics.

Figure 28 shows the distributions with respect to the square of the mass of the pions, kaons, and protons in the momentum range 12.9–25.9 GeV/c. Figure 29 shows one of the events of $K\to\mu\nu$ decays detected in SKOCh.

The apparatus made it possible to detect several signals from each hodoscope photomultiplier during a total drift time of $T_0 = 300$ nsec (during one triggering). An illustration of its use is Fig. 30, which shows an event corresponding to the passage of two particles simultaneously through SKOCh. Such events were selected by a trigger that used information from the drift chambers and scintillation counters at the entrance to SKOCh. The use of many-particle detecting electronics makes it possible to simplify the reconstruction of events with several rings in the spectrometer and also increase the number of detected points.

A method for detecting rings using this optical scheme and straight arrangements with discrete photomultipliers is

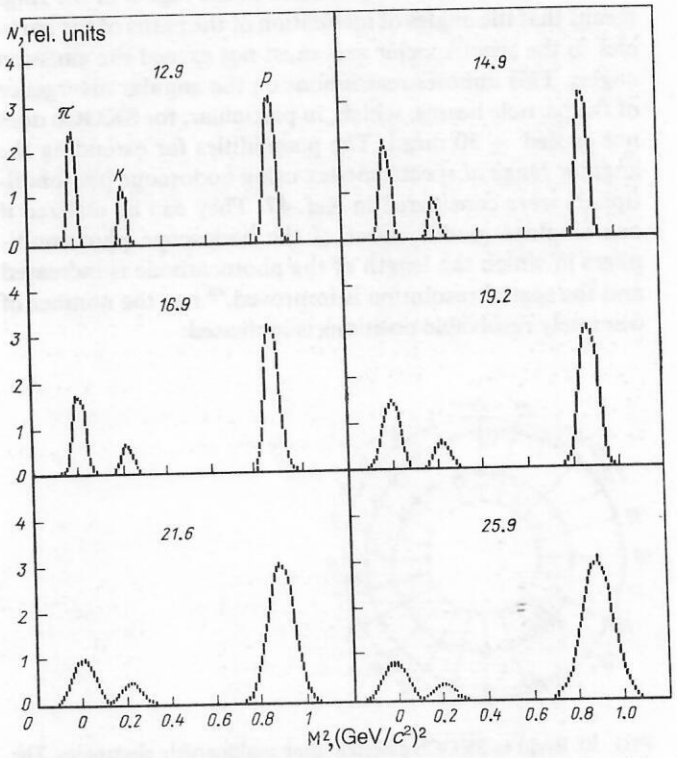

FIG. 28. Distributions with respect to the squares of the masses of the particles.

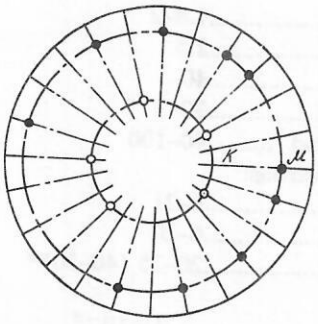

FIG. 29. An event of $K \to \mu\nu$ decay,

also being developed at Serpukhov. The first such spectrometer was used in an experiment to look for new stable particles in the region of masses up to 2 GeV/c^2 (Ref. 45). Later, the spectrometer was modified[46] for experiments in the hyperon beam of the Serpukhov accelerator. The optical scheme of the modification is shown in Fig. 31. In the detecting system there are 20 one-dimensional photon detectors, each with 16 photomultipliers (FÉU 85). The discretization step in the line of detectors is 5 mm. For a gas radiator of length 1.5 m (2 atm pressure of SF_6) and focal length 4 m of the spherical mirror, a velocity resolution $\Delta\beta/\beta = 1.5\times10^{-5}$ and $N_0 = 40$ were obtained. The detector works reliably in the immediate vicinity of the target, onto which a slowly extracted proton beam is directed (the load at the position of the detector is up to 10^7 sec^{-1}).

Some features of these optical schemes relating to the range of angles of the detected particles should be noted. It is readily seen that the angular accuracy and the accuracy with which the ring radii are measured are less good if the ring extends beyond the center of the employed coordinate system, i.e., the center of the focal plane. The condition for the center of the system to be situated in the region of the rings means that the angles of inclination of the paths of the particles to the spectrometer axis must not exceed the emission angles. This imposes restrictions on the angular divergence of the particle beams, which, in particular, for SKOCh does not exceed $\pm$ 30 mrad. The possibilities for extending the angular range of spectrometers using hodoscope photomultipliers were considered in Ref. 47. They can be realized if one employs modifications of the hodoscope photomultipliers in which the length of the photocathode is increased and the spatial resolution is improved,[48] i.e., the number of discretely resolvable positions is increased.

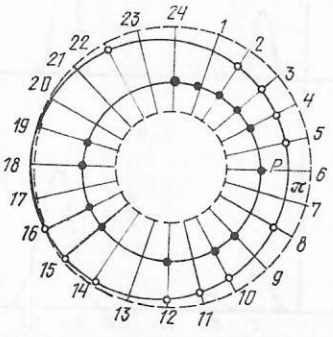

FIG. 30. Event in SKOCh detected using multiparticle electronics. The channels with numbers 2, 3, 4, 10, 12, 15, and 16 each responded twice to a single triggering.

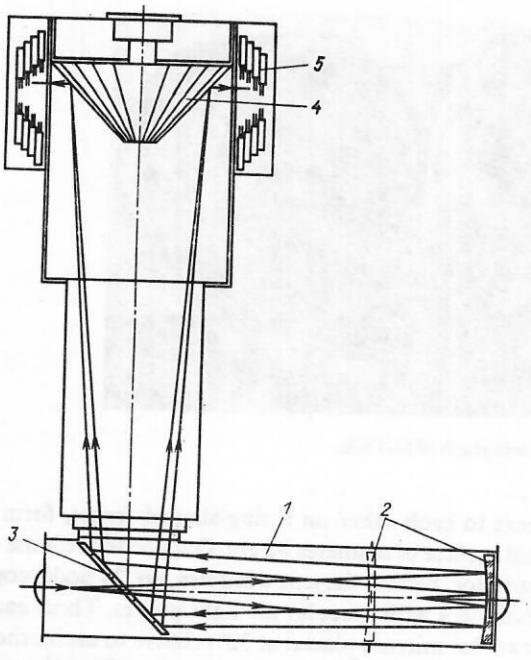

FIG. 31. Optical scheme of multichannel Cherenkov detector: 1) radiator; 2) spherical mirror; 3) flat mirror; 4) reflector; 5) photomultipliers.

To detect particles in a wide range of angles, one can use an approach based on Schluter's proposal.[49,50] In this case, a fiber-optic disk is placed in the focal plane of the spherical mirror and used to direct the light onto the photon detectors. It was shown by a calculation in Ref. 47 that for a photon detector comparable in size and spatial resolution to the one used in the experiment E 605 (Refs. 17 and 18) one needs 200 hodoscope photomultipliers in conjunction with fiber optics.

One can say that the method of detecting rings using vacuum photodetectors is far from the full exploitation of its potential. New possibilities are opened up by the introduction of multianode position-sensitive arrangements. In addition, there are possibilities in the use of miniaturized photomultipliers and also new modifications of the hodoscope photomultipliers. An advantage of the latter is the possibility of replacing one device by several tens of individual miniaturized photomultipliers.

3. DEVELOPMENTS AND PROSPECTS OF THE METHOD

We consider developments aimed at eliminating the shortcomings of chamber-based photon detectors. We saw that the main shortcomings of multistage proportional chambers used as photon detectors are the impossibility of multiparticle detection and the relatively low quality. The study of Ref. 51 was devoted to elimination of these shortcomings. Photon detectors are shown in Fig. 32. Instead of the gap of the proportional chamber, a plane-parallel grid electrode with a cathode electrode near it is used. A natural way of eliminating the ambiguity in the determination of the coordinates of the photons is to divide the cathode electrode into areas. In the given construction, a cathode electrode divided into three zones is used (Fig. 33b). Using a method of "weights and strips" in the indicated configurations of the electrode (Fig. 33a) (individual area), one can attain a spatial accuracy in determining a photon coordinate of 0.4 mm. The chamber was tested with a filling of methane or isobu-

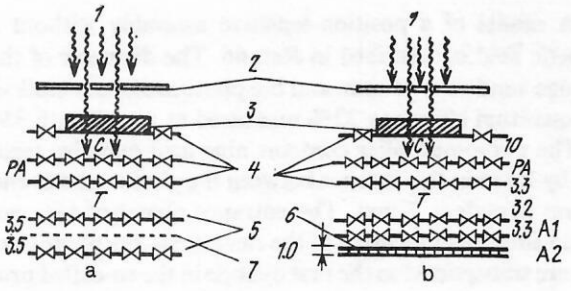

FIG. 32. Schematic arrangement of photon detectors (dimensions given in mm): a) variant of ordinary multistage chamber; b) plane-parallel gaps A_1 and A_2 are used in the region of the proportional chamber; 1) parallel beams of photons; 2) masks; 3) windows; 4) grid electrodes; 5) grids; 6) printed circuit with readout electrode; 7) proportional chamber.

tane at pressures in the range 5–20 mm Hg with saturated TMAE vapor (partial pressure 0.3–0.7 mm Hg, $T = 20$–$30\,^{\circ}C$). The total gas multiplication was 2×10^6. The best coordinate accuracy (0.4 mm) was obtained with isobutane. Operation of the chamber at low pressure sharply reduces its sensitivity to charged particles. The use of isobutane in conjunction with intermediate transport almost completely suppresses the optical feedback. The use of TMAE to increase N_0 makes it necessary to increase the conversion interval, but the authors hope to use the difference in the electron conversion times to improve the conditions of multiphoton detection.

With regard to the improvement of the characteristics of two-coordinate drift chambers as photon detectors, great efforts are being devoted to improving the spectral properties of the elements of the optics, and also to eliminate the shortcomings noted above.[52,53] There are a number of developments associated with different methods of information readout from the photon detectors. They relate to the use of cathode electrodes made in the form of areas, the current-division method, etc.

Some developments concern other constructive solutions for photodetectors. In Ref. 54, Comby *et al.* report a test of a needle counter.

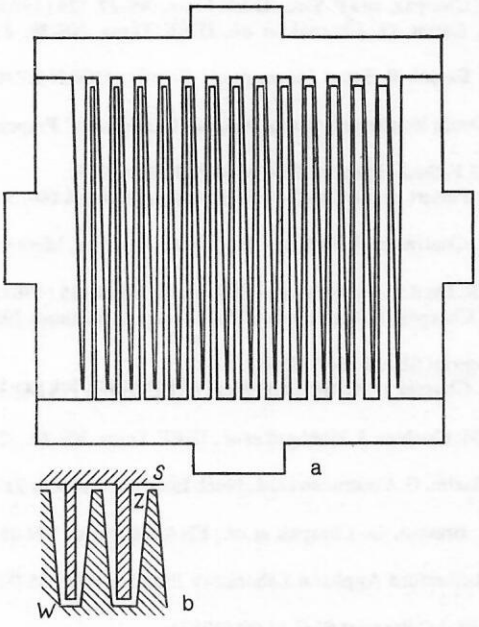

FIG. 33. Structure of electrode (a) and schematic representation of S, Z, and W electrodes (b).

Two modifications were tested—with 1024 needles forming a 32×32 matrix with 3-mm spacing, and with 2500 needles placed at the vertices of equilateral triangles of side 3 mm. The main results refer to the first construction. Surgical steel needles with tips of radius 12 ± 3 μm were used. The cathode plane was a copper plate of thickness 2 mm with round openings at the positions of the tips of the needles. The tips were 0.3 mm below the cathode plate. A MgF_2 window with a first grid electrode pressed tightly to its surface was used. The chamber was filled with a mixture of argon and TEA, and also methane and TEA. A plateau in the counting characteristic for individual photons and a value $N_0 = 28$ in a beam of pions with momentum 6 GeV/c were obtained. The gas radiator was a volume of argon with length 93 cm along the beam at atmospheric pressure. The time of stable operation of the needles was studied. After 3×10^9 responses of an individual needle, the detection efficiency was reduced by a factor of two. Examination under a microscope showed that the reason for the decrease in the efficiency was crystalline formations on the tip of the needles. After washing in spirit, the efficiency was restored.

The advantages of needle counters as photon detectors are the high amplification, the absence of ambiguity in the determination of the coordinates of the photons, and the short duration of the signal, since the discharge occurs in a region near the tip of the needle. However, serious difficulties arise in their construction due to the high accuracy required in the mutual positioning of the electrodes (a few tens of microns over a base of hundreds of millimeters). As in the case of discrete vacuum photon detectors, there is a natural difficulty in the information readout—the large number of channels. In the early studies,[55] a delay line with distributed resistance was used in order to economize on the electronics. Despite the poorer load characteristics, the authors regarded this direction as promising.

We should now mention the developments relating to ring detection by means of chambers operating in a high-current regime.[56] The main advantages of the method are the high gas multiplication and the simplification in connection with this of the photon detection conditions, and also the fairly high counting rate in the case of large chambers. The main difficulty arises from the following circumstances. For efficient detection of the photons, it is necessary to have good conversion of them into photoelectrons in a gas medium, but stable operation of a chamber in a high-current regime requires the opposite—effective absorption of the photons during gas multiplication. We note that in such a regime additives that absorb the vacuum ultraviolet are usually employed in the chambers. In a study made at Serpukhov it was shown[57] that one can realize conditions that meet simultaneously the two requirements which we have noted. Investigations of the method are continuing.

We also mention developments relating to attempts to detect photons in a gas medium using photocathodes.[58] The main aim of these developments is to replace the photosensitive additives (like TEA and TMAE) by the photoemission layers used in vacuum photon detectors, all the possibilities of the chamber method being preserved. The main difficulties of the method are due to the lower photoemission from photocathodes into a gas medium compared with vacuum, and also the degradation of the photocathodes in the atmo-

sphere of the organic additives used in the chambers. It was shown, however, that in an atmosphere of noble gases at low pressure (a few millimeters of mercury) one can obtain an appreciable yield from a bialkali photocathode (about 10%) and simultaneously a gas multiplication $\simeq 50$.[59] In a further study,[60] an attempt was made to realize the method using CsI. We can also mention Ref. 61, where it is noted that in a multistage proportional chamber with cathode readout it proved possible to obtain simultaneously an appreciable emission from the photocathode and gas multiplication.

We also consider the possible use of fiber optics for detection of Cherenkov ring radiation. This is justified in systems with image reduction. Besides this, it is possible to reduce the number of detection channels by using the standard information coding methods of fiber optics. Finally, it is in principle possible to develop photon detectors in which light amplification intervals are used before the fiber-optic disk (for example, multiplication of electrons in a gas medium with subsequent detection of the electroluminescence).

In conclusion, we consider developments associated with the creation of multianode vacuum photon detectors. We first consider the developments in which a structure is used: photocathode–microchannel-plate amplification cascade (Ref. 62)–multianode matrix. In Ref. 63, there is a description of a photomultiplier with a matrix of 400 anodes separated by a spacing of 0.65 mm. The sensitive area of the assembly is 12×16 mm^2. A bialkali photocathode (quantum efficiency 18% at wavelength 430 nm) and two microchannel-plate amplification cascades are used. The assembly is fitted into a frame with outer diameter 24.9 mm. The following characteristics are given: resolution $\sigma_{XY} = 0.6$ mm, photomultiplier gain 10^4–10^5, signal rise time 0.6 nsec. There are other similar developments, differing in the constructional implementation.[64] We must, however, mention the general shortcomings of vacuum photon detectors using microchannel plates as multiplying systems. They include an appreciable dark current, saturation effects that limit the counting rate, and degradation of the secondary-emission layers over which the potential is distributed.[63]

These phenomena can be suppressed to a large degree if one uses in the assemblies multiplication systems constructed in accordance with the principle of discrete dynodes. In Ref. 65 there is a description of a photomultiplier with discrete dynodes and a sectioned anode. The photomultiplier has a window of diameter 20 mm, a bialkali photocathode, ten dynodes separated by ceramic rings, and an anode constructed in the form of a matrix of 4×4 areas. The size of each area is 2.6×2.6 mm^2, and the gap between them is 0.3 mm. Each of the ten dynodes contains two planes of electrodes of triangular section measuring 0.5 mm along the base, the electrodes being separated by 0.5 mm. The electrodes in each dynode plane are staggered by a small distance to eliminate the optical and ion feedback. The shape of the electrodes and the electric field configuration were optimized with a view to ensuring a high coefficient of secondary emission of electrons. The measured parameters of the photomultiplier are as follows: quantum efficiency 20%, gain 10^6, and spatial resolution ± 1.7 mm with respect to the X and Y coordinates. Good stability of the parameters was noted. An axial magnetic field was used in this photomultiplier to focus the electrons.

A model of a position-sensitive assembly without a magnetic field is described in Ref. 66. The diameter of the entrance window is 75 mm, and the photocathode is bialkali with quantum efficiency 22% measured at wavelength 350 nm. The photomultiplier contains nine grid dynodes separated by 1.3 mm; the distance between the photocathode and the first dynode is 7 mm. The entrance chamber does not contain additional focusing of the electrons—the photoelectrons are transported to the first dynode in the so-called projective geometry. The anode contains ten wire electrodes. The spatial resolution measured in the direction perpendicular to the electrodes was ± 3 mm, the gain of the photomultiplier 10^5, and the signal duration at its base 15 nsec. At total voltage 1000 V, the photomultiplier was found to be weakly sensitive to an external magnetic field because of the close spacing of the grid electrodes. Developments of photomultipliers with discrete dynodes and matrices of 32×32 anodes are currently being made by the firm Phillips.

This direction in the development of photon detectors is obviously very promising. The construction of large-area multianode assemblies with high spatial resolution may open up new possibilities of vacuum photon detectors for Cherenkov ring radiation detection.

[1)] *Translator's Note.* The Russian notation for the trigonometric, inverse trigonometric, hyperbolic functions, etc., is retained here and throughout the article in the displayed equations.

[2)] In this case, a spherical mirror is not used, and the Cherenkov radiation cone, emerging from the thin radiator, impinges directly on the photon detector.[25]

[1] G. Arnison, B. Astbury, B. Aubert *et al.*, Phys. Lett. **122B**, 103 (1983).
[2] M. Banner, Ph. Bloch, F. Bonaudi *et al.*, Phys. Lett. **122B**, 476 (1983).
[3] "Technical proposal DELPHI," CERN Preprints LEPC/83-3, LEPC 32 (1983).
[4] J. Seguinot and T. Ypsilantis, Nucl. Instrum. Methods **142**, 377 (1977).
[5] J. Sequinot, J. Tocqueville, and T. Ypsilantis, Nucl. Instrum. Methods **173**, 283 (1980).
[6] D. Anderson, Nucl. Instrum. Methods **178**, 125 (1980).
[7] B. Yu. Baldin, Yu. N. Vrazhnov, S. I. Bytukov *et al.*, Nucl. Instrum. Methods **140**, 409 (1977).
[8] G. Melchart, G. Charpak, and F. Sauli, IEEE Trans. **NS-27**, 124 (1980).
[9] A. Breskin, A. Cattai, G. Charpak *et al.*, IEEE Trans. **NS-28**, 429 (1981).
[10] E. Barrelet, T. Ekelof, B. Lund Jensen *et al.*, Preprint CERN-EP/09 (1982).
[11] J. Sequinot, "Cours lecture series, ring imaging Cherenkov," Preprint CERN (1982).
[12] G. Charpak and F. Sauli, Preprint CERN-EP/83-128 (1983).
[13] G. Charpak, A. Peisert, and F. Sauli, Nucl. Instrum. Methods **180**, 387 (1981).
[14] Ph. Mangeot, J. Coutracon, J. Hubbard *et al.*, Nucl. Instrum. Methods **216**, 79 (1983).
[15] M. Davenport, R. Deol, P. Flower *et al.*, IEEE Trans. **NS-30**, 35 (1983).
[16] R. Bouclier, G. Charpak, A. Cattai *et al.*, Nucl. Instrum. Methods **205**, 403 (1983).
[17] S. Williams, Preprint SLAC-3360 (1984).
[18] R. Bouclier, G. Charpak, J. C. Santiard *et al.*, IEEE Trans. **NS-30**, 30 (1983).
[19] G. Coutracon, M. Criebier, J. Hubbard *et al.*, IEEE Trans. **NS-29**, 323 (1982).
[20] M. Adams, A. Bastin, G. Coutracon *et al.*, Nucl. Instrum. Methods **217**, 237 (1983).
[21] R. Bouclier, A. Breskin, G. Charpak *et al.*, FNAL Preprint FN-351 (1981).
[22] G. Hallewell, Rutherford Appleton Laboratory Preprint RAL 85-009 (1984).
[23] R. Baltrusaitis, SLAC Preprint SLC-Ll-09 (1982).
[24] V. Ashford, T. Bienz, F. Bird *et al.*, Preprint SLAC-3772 (1985).

[25]P. A. Cherenkov, I. E. Tamm, and I. M. Frank, *Nobel Lectures* [in Russian] (Fizmatgiz, Moscow, 1960).
[26]M. M. Butslov, M. N. Medvedev, I. V. Chuvilo, and M. V. Sheshunov Nucl. Instrum. Methods **20**, 263 (1963).
[27]S. P. Denisov, Preprint 71-74 [in Russian], Institute of High Energy Physics, Serpukhov (1971).
[28]Yu. P. Gorin, S. P. Denisov, S. V. Donskov *et al.*, Nucl. Instrum. Methods **92**, 77 (1971).
[29]N. Giordenescu, V. N. Zubarev, V. I. Ivanov *et al.*, Preprint RI-5460 [in Russian], JINR, Dubna (1970).
[30]M. Benot, J. Bertrand, A. Maurer *et al.*, Nucl. Instrum. Methods **165**, 439 (1979).
[31]R. Meunier, Preprint CERN EP/85-16 (1985).
[32]R. Giese, O. Gildemeister, W. Paul, and G. Schuster, Nucl. Instrum. Methods **88**, 83 (1970).
[33]B. Robinson, Phys. Scr. **23**, 716 (1981).
[34]T. Gooch, R. Gilmore, D. Jeffery *et al.*, Nucl. Instrum. Methods **A241**, 363 (1985).
[35]N. K. Vishnevskiĭ, R. K. Krasnokutskiĭ, V. G. Lapshin *et al.*, in: *Proc. of the International Conference on Instruments in High Energy Physics*, D5805 [in Russian] (JINR, Dubna, 1970), p. 305.
[36]N. F. Aleksandrova, N. K. Vishnevskiĭ, O. S. Korol'kova *et al.*, Preprint 69-22 [in Russian], Institute of High Energy Physics, Serpukhov (1969).
[37]V. G. Vasil'chenko, V. G. Lapshin, E. A. Monich *et al.*, Prib. Tekh. Eksp. No. 4, 183 (1978).
[38]Yu. D. Karpekov and V. I. Solyanik, Preprint 77-35 [in Russian], Institute of High Energy Physics, Serpukhov (1977).
[39]B. Yu. Baldin, L. S. Vertogradov, N. K. Vishnevskiĭ *et al.*, Yad. Fiz. **20**, 694 (1974) [Sov. J. Nucl. Phys. **20**, 371 (1975)].
[40]V. V. Abramov, A. V. Alekseev, B. Yu. Baldin *et al.*, Nucl. Instrum. Methods **A235**, 497 (1985).
[41]V. V. Abramov, A. V. Alekseev, B. Yu. Baldin *et al.*, Preprint 81-46 [in Russian], Institute of High Energy Physics, Serpukhov (1981).
[42]Yu. B. Bushnin, A. A. Denisenko, A. F. Dunaĭtsev *et al.*, Preprint 77-84 [in Russian], Institute of High Energy Physics, Serpukhov (1977).
[43]B. Yu. Baldin, Prib. Tekh. Eksp. No. 5, 137 (1980).
[44]S. I. Bityukov, B. Yu. Bushnin, R. I. Dzhelyadin *et al.*, in: *Proc. of the International Symposium on Wire Chamber Methods*, D13-9164 [in Russian] (JINR, Dubna, 1975), p. 24.
[45]V. G. Vasil'chenko, F. D. Vlatskiĭ, S. A. Zelepukin *et al.*, Preprint 79-84 [in Russian], Institute of High Energy Physics, Serpukhov (1979).
[46]G. A. Akopdzhanov, Yu. L. Grishkin, V. F. Kuzichev *et al.*, Preprint 86-10 [in Russian], Institute of High Energy Physics, Serpukhov (1986).
[47]B. Yu. Baldin, V. G. Vasil'chenko, A. A. Volkov *et al.*, Preprint 85-40 [in Russian], Institute of High Energy Physics, Serpukhov (1985).
[48]V. G. Vasil'chenko, A. G. Daĭkovskiĭ, V. G. Lapshin *et al.*, Preprint 77-116 [in Russian], Institute of High Energy Physics, Serpukhov (1977).
[49]R. A. Schluter, in: *Proc. of the Intern. Conf. on High Energy Physics* (New York, 1961), p. 91.
[50]V. P. Zrelov, *Cherenkov Radiation and its Use in High Energy Physics*, Vol. 2 [in Russian] (Atomizdat, Moscow, 1968).
[51]W. Dominik, D. Anderson, A. Breskin *et al.*, Preprint CERN EP/84-29 (1984).
[52]P. Leith, Preprint SLAC-3829 (1985).
[53]A. Peisert, Preprint CERN-EP/8206 (1982).
[54]G. Comby, J. Chalot, J. Quidort, and A. Zadra, IEEE Trans. **NS-29**, 328 (1982).
[55]R. Grove, K. Lee, V. Perez-Mendez, and J. Sperinde, Nucl. Instrum. Methods **89**, 257 (1970).
[56]G. D. Alekseev, V. V. Kruglov, and D. M. Khazins, Fiz. Elem. Chastits At. Yadra **13**, 703 (1982) [Sov. J. Part. Nucl. **13**, 293 (1982)].
[57]A. F. Buzulutskov, V. G. Vasil'chenko, V. Yu. Vashchenko *et al.*, Preprint 84-108 [in Russian], Institute of High Energy Physics, Serpukhov (1984).
[58]G. Kneller, Preprint CERN-EP/83-34 (1983).
[59]G. Charpak, W. Dominik, S. Majevski, and F. Sauli, IEEE Trans. **NS-30**, 134 (1983).
[60]S. Williams, P. Leith, M. Poppo, and T. Ypsilantis, IEEE Trans. **NS-27**, 91 (1980).
[61]F. Sauli, Preprint CERN-EP/82-26 (1982).
[62]C. Lo, P. Lecomt, and B. Lescovar, IEEE Trans. **NS-24**, 302 (1977).
[63]K. Oba, M. Sugiyama, Y. Suzuki, and Y. Yoshimura, IEEE Trans. **NS-26**, 346 (1979).
[64]R. Meunier and A. Maurer, IEEE Trans. **NS-25**, 528 (1978).
[65]K. Kuroda, Nucl. Instrum. Methods **196**, 187 (1982).
[66]H. Kume, S. Suzuki, K. Oba, and J. Takeuchi, IEEE Trans. **NS-32**, 355, 448 (1985).
[67]M. Salomon and S. Williams, Nucl. Instrum. Methods **A241**, 210 (1985).

Translated by Julian B. Barbour